Macromolecules

pubs.acs.org/Macromolecules Article

Depolymerization of P(PDMS$_{11}$MA) Bottlebrushes via Atom Transfer Radical Polymerization with Activator Regeneration

Michael R. Martinez, Sajjad Dadashi-Silab, Francesca Lorandi, Yuqi Zhao, and Krzysztof Matyjaszewski*

Cite This: *Macromolecules* 2021, 54, 5526−5538 Read Online

ACCESS | Metrics & More | Article Recommendations | Supporting Information

ABSTRACT: Depolymerization of vinyl polymers into monomers is energy-intensive due to the high thermal and chemical stability of the backbone. Depolymerizations of methacrylic polymers are typically conducted above the ceiling temperature and thermal degradation temperature to degrade polymers by bond scission. This work investigates the catalyzed depolymerization of a Cl-capped poly(poly(dimethylsiloxane) methacrylate) (P(PDMS$_{11}$MA-Cl)) polymer mediated by an atom transfer radical polymerization catalyst: copper(II) chloride/tris(2-pyridylmethyl)-amine ($CuCl_2$/TPMA) at 170 °C. The depolymerization yield, rate, and selectivity were improved by increasing the ratio of [TPMA]/[$CuCl_2$]. Electron transfer from the ligand contributed to the Cu(I) activator (re)generation at high temperature (T > 130 °C), as proven by ultraviolet−visible spectroscopy. The bottlebrush could be partially depolymerized and repolymerized over a few cycles.

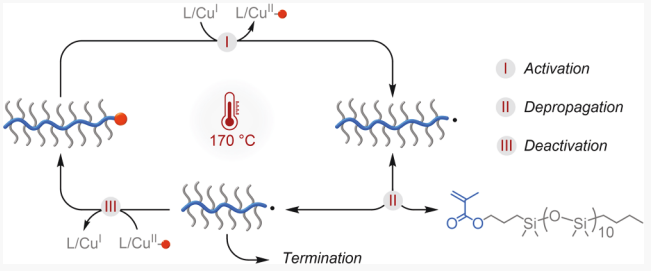

INTRODUCTION

Over 8.3 billion metric tons of plastic was produced since the 1950s, yet only 9% has been recycled.[1] Most of the recycled plastics lose value due to issues in mechanical processing or contamination with other chemicals during the recycling process.[2,3] This is especially problematic for high-value/high-performance plastics, which lose most of their outstanding qualities after recycling. These inefficiencies in waste disposal and recycling methods prompt development of new chemical recycling methods, which can contribute to a circular polymer economy.

Chemical recycling involves depolymerization, isolation, and implementation of plastic waste to make new materials with an equal or greater value.[4−8] Chemical recycling can decompose plastic waste into feedstocks, which can be used to create value-added polymers.[2,4,9,10] Chemically degradable, "self-immolative" materials are designed to mimic the material properties of high-performance polymers but possess functionalities that can trigger depolymerization of the polymer.[6,11] Depolymerization is also enhanced by instability between repeat units and can be induced by bond scission.[5,6] Catalysts can be used to start or alter the product distribution of depolymerization reactions.[4−7]

The applicability of a depolymerization driven by depropagation depends on the monomer's thermodynamics of polymerization. The enthalpy (ΔH) and entropy (ΔS) of chain growth polymerizations are typically negative.[12−15] The free energy of a polymerization (ΔG) under nonstandard state conditions would follow $\Delta G = \Delta H - T(\Delta S^\circ + R\ln([M]_0/c^\circ))$ (ΔS° is standard-state entropy, c° is 1 mol dm^3, and $[M]_0$ is the initial monomer concentration).[13,15−17] Propagation is favored at ΔG < 0, depropagation is favored at ΔG > 0, and the equilibrium between propagation and depropagation is established when ΔG = 0 at the ceiling temperature (T_c). The standard Gibbs energy is related to the equilibrium constant (K_{eq}) at the equilibrium monomer concentration ($[M]_{eq}$) by eqs 1 and 2 when ΔG = 0.[15] K_{eq} is the ratio of the rate constant of propagation (k_p) to the rate constant of depropagation (k_{dp}).

$$\Delta G^\circ = -RT\ln K_{eq} \quad (1)$$

$$K_{eq} = k_p/k_{dp} = 1/[M]_{eq} \quad (2)$$

An ideal living polymerization will favor propagation until the rate of propagation equals the rate of depropagation at the $[M]_{eq}$. Activation of a dormant polymer can favor depropagation until equilibrium is reached at the $[M]_{eq}$ if other products are not formed.[18−21]

Polymers with aliphatic backbones have high chemical and thermal stability. Depolymerization of poly(methyl methacrylate) (PMMA) is of high interest due to its broad industrial applications and relatively low T_c(bulk) = 296 °C and $T_c(c^\circ)$ = 205 °C.[22−27] Thermal depolymerization of PMMA can be induced by bond scission of weaker bonds (head−head bonds or unsaturated chain ends) at lower temperature or by random bond scission and unzipping at higher temperature.[26,28−32]

Received: February 22, 2021
Revised: May 15, 2021
Published: June 1, 2021

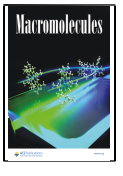

https://doi.org/10.1021/acs.macromol.1c00415
Macromolecules 2021, 54, 5526−5538

Inhibitors or a loss of chain-end functionalities (CEFs) due to termination can prevent depolymerization of methacrylates by radical mechanisms under mild conditions.[33−35] Dilute depolymerizations of PMMA were induced by bond scission of weak links at 236 °C at 1 w/v% concentration. These depolymerizations recovered ∼10−35% of the monomer and stopped once the chain end was terminated by transfer to the solvent.[33,34] Thermolysis of PMMA at higher temperature could recover a larger monomer fraction but may degrade high-value PMMA into soot and other impurities.[23,36] Advances in pyrolysis technology enabled >97% MMA monomer recovery at T > 350 °C.[24,26] A compromise between energy efficiency and selectivity may plausibly be reached by mediating the depolymerization by a living process closer to the T_c.

Reversible deactivation radical polymerization (RDRP) endows polymer chains with CEFs, which can be utilized for chain extensions or to trigger depolymerization reactions, with the propensity for propagation or depropagation determined by the thermodynamics of the system. Deactivation of a polymer chain in RDRP can be through a reversible addition−fragmentation chain-transfer (RAFT) mechanism regulated by a chain-transfer agent (CTA), by reversible deactivation in a nitroxide-mediated polymerization, or by reversible halogen atom transfer between a catalyst (often copper, ruthenium, or organic photocatalysts) and the radical chain end in an atom transfer radical polymerization (ATRP).[37−40]

In ATRP, the equilibrium between the alkyl halide initiator or halogen-capped dormant species (P_n-X) and the reduced Mt^n/L with the chain-end radical ($P_n^{\cdot}$) and the oxidized X-Mt^{n+1}/L catalyst (Mt = transition metal, L = ligand) strongly favors the oxidized species (Scheme 1).[41] Biradical termination is diminished by the persistent radical effect.[42] Thus, the CEF is preserved, and the macroinitiator can be used for chain extensions and post-synthetic modifications. The Mt^n/L activator catalyst can be (re)generated by employing a reducing agent to reduce the X-Mt^{n+1}/L deactivator in an activator regenerated by electron transfer (ARGET) process.[43] Similarly, an external radical source could also regenerate Mt^n/L.[44] Regeneration of the Mt^n/L activator enables control over polymerizations at parts per million (ppm) catalyst loadings with high retention of alkyl halide CEFs.[45]

Scheme 1. General Scheme of ATRP with Catalyst Regeneration and Propagation/Depropagation Equilibria

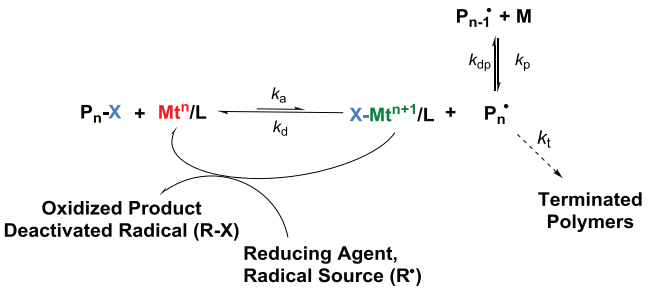

High-T_c poly(acrylamides) and poly(acrylates) were depolymerized by an unknown mechanism in the presence of a copper(II) bromide/tris[2-(dimethylamino)ethyl]amine (Me_6TREN) catalyst in CO_2-saturated water.[46] Monomer recoveries as high as 71% were achieved at low temperature.

Partial depolymerization of PMMA mediated by ATRP with a Ru catalyst was recently reported.[18] Initial concentrations were varied from 0.5 to 10 mM within a temperature range of 60 to 120 °C. Reiterative cycling by evaporation allowed for successive depolymerizations of the chain end to reach an ∼15% MMA yield after four cycles.

Methacrylic macromonomers have less favorable thermodynamics and a lower repeat unit concentration than MMA, which enabled depolymerization of poly(macromonomer) bottlebrushes into macromonomers to significantly higher yields.[35,47] The partial depolymerization of oligo(ethylene oxide) methacrylate (OEOMA) and poly(dimethylsiloxane) methacrylate (PDMSMA) poly(macromonomers) was initiated at 60 °C at an initial repeat unit concentration ($[P]_0$) of 0.1 M by thermolysis of a RAFT CTA-capped chain end.[35] The bottlebrush depolymerized until ∼30% macromonomer was recovered at the $[M]_{eq}$ of ∼30 mM. The methacrylate-functionalized polyhedral oligomeric silsesquioxane (iBuPOSSMA) macromonomer was polymerized to ∼80% monomer conversion by ATRP at 60 °C via a grafting-through approach and depolymerized to ∼60% monomer conversion by increasing the reaction temperature to 90 °C in one pot.[47]

This manuscript describes the depolymerization of a chlorine-capped poly(poly(dimethylsiloxane) methacrylate) (P-($PDMS_{11}$MA)-Cl) by ATRP catalyzed by a $CuCl_2$/tris(2-pyridylmethyl)amine ($CuCl_2$/TPMA) catalyst at 170 °C. P($PDMS_{11}$MA) bottlebrushes have broad applications as supersoft elastomers with moduli on the order of 1 kPa.[48−50] In this manuscript, P(PDMSMA)-Cl is used as a model compound for bulky methacrylate depolymerization by ATRP at elevated temperature. Depolymerizations were conducted at the high end of the extrapolated range of T_c for similarly sized PDMSMA macromonomers found by RAFT and AGET ATRP in dioxane (T_c = 147 to 181 °C, $[M]_0$ = 0.1−480 mM).[35,51] Control experiments suggest that the depolymerization reactions were catalyzed by the atom transfer radical polymerization process. Depolymerizations were accelerated with higher catalyst concentrations and a larger excess of the TPMA ligand,

Table 1. Properties of the $PDMS_{11}$MA Macromonomer and Bottlebrushes before/after Incubation at 170 °C under Nitrogen

sample[a]	$M_{n,app}$[b]	$Đ$[b]	f (%)[c]	$T_{d,5\%}$[d]	$T_{d,10\%}$[d]	$T_{d,50\%}$[d]
$PDMS_{11}$MA	1108	1.21	98	183	210	287
$PDMS_{11}$MA-heat	1122	1.20	97	186	212	285
P($PDMS_{11}$MA)$_{38}$-Cl	16,840	1.13	<1	286	332	379
P($PDMS_{11}$MA)$_{38}$-Cl-heat	16,830	1.15	<1	261	284	353
P($PDMS_{11}$MA)-RP	290,000	2.62	3	256	269	319
P($PDMS_{11}$MA)-RP-heat	300,000	2.68	4	250	280	337

[a]Incubated samples are denoted with the postscript "-heat". Samples were incubated at 170 °C under nitrogen for 2 h. [b]Measured by GPC relative to linear PMMA standards in THF. [c]The mole fraction of vinyl products, taken as the ratio of vinyl proton signals (δ = 5.56 and 6.12, singlets) to O−CH_2 signals (δ = 3.8−4.40, broad) by ^{1}H NMR. [d]Thermal decomposition temperatures in °C, given at 5, 10, and 50 wt % mass loss by TGA.

https://doi.org/10.1021/acs.macromol.1c00415
Macromolecules 2021, 54, 5526−5538

such that ~80% macromonomer could be recovered in 10 min. Model reduction experiments showed that the catalyst was reduced through electron transfer reactions with the ligands, which can act as electron donors.

RESULTS AND DISCUSSION

Bottlebrush Synthesis and Thermogravimetric Analysis. A P($PDMS_{11}MA$)-Cl brush polymer was prepared by ARGET ATRP of a poly(dimethylsiloxane) methacrylate macromonomer ($PDMS_{11}MA$) with an ethyl chlorophenyl acetate (EClPA) initiator, a $CuCl_2$/TPMA catalyst, and a $Sn(EH)_2$ reducing agent at 60 °C. The polymerization used molar ratios $[PDMS_{11}MA]_0/[EClPA]_0/[CuCl_2]_0/[TPMA]_0/[Sn(EH)_2]_0$ = 25/1/0.05/0.075/0.0265 at $[PDMS_{11}MA]_0$ = 500 mM in chlorobenzene and was stopped at 72% conversion to preserve a high CEF.[49] The residual macromonomer was removed by fractionation to yield a purified P($PDMS_{11}MA$)$_{38}$-Cl bottlebrush with <1% macromonomer impurity. The length of the P($PDMS_{11}MA$)$_{38}$-Cl macroinitiator was determined to be 38 by integration of methylene protons in the side chain relative to the EClPA phenyl protons by ^{1}H NMR (Figure S1).

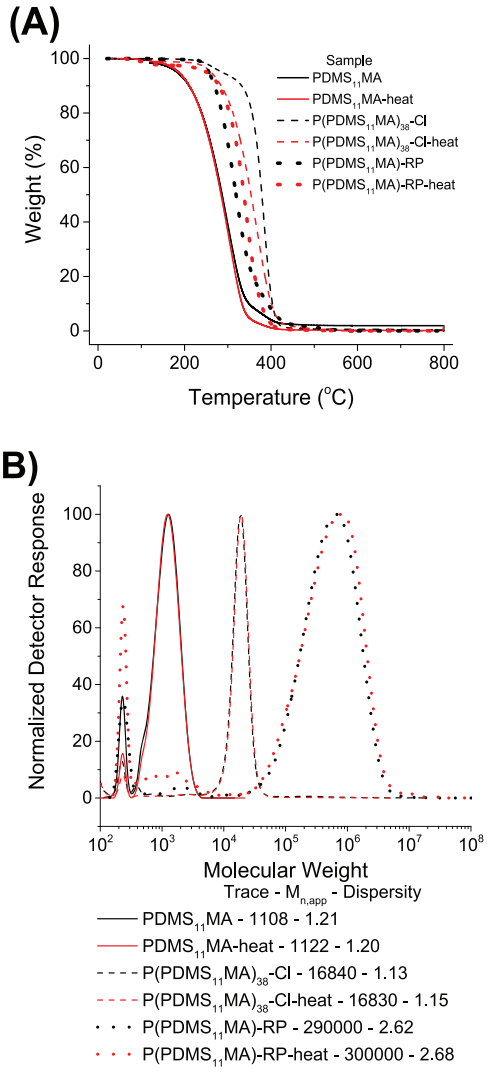

Figure 1. (A) TGA of $PDMS_{11}MA$ and P($PDMS_{11}MA$) samples before and after incubation at 170 °C under a nitrogen atmosphere. Incubated samples are denoted with the postscript "-heat". TGA experiments were conducted under nitrogen at a heating rate of 10 °C/min. (B) GPC traces of purified and incubated polymer samples. Molecular weight is given relative to linear PMMA standards in THF. The peak at M_p = 227 is a diphenyl ether internal standard used for GPC calibration.

Thermal stability of $PDMS_{11}MA$ and P($PDMS_{11}MA$)$_{38}$-Cl was assessed by ^{1}H NMR, gel permeation chromatography (GPC), and thermogravimetric analysis (TGA) after incubation at 170 °C for 2 h (Table 1). TGA of the incubated and pure $PDMS_{11}MA$ followed a one-step mass loss beginning at ~150 °C (Figure 1A and Figure S2A). The ^{1}H NMR spectra showed that the vinyl protons were intact and the macromonomer did not polymerize after incubation (Figures S3 and S4). There was a decrease in low-molecular-weight polymer peak intensity in the GPC traces, resulting in a slight increase in $M_{n,app}$ and a decrease in dispersity ($Đ$) after incubation (Figure 1B). Thus, $PDMS_{11}MA$ is stable at 170 °C.

^{1}H NMR of P($PDMS_{11}MA$)$_{38}$-Cl and incubated P($PDMS_{11}MA$)$_{38}$-Cl-heat confirmed that P($PDMS_{11}MA$)$_{38}$-Cl did not depolymerize in the absence of a catalyst after incubation at 170 °C (Figure S5). This was supported by nearly identical GPC traces before and after incubation (Figure 1B). However, there were significant differences in thermal stability between the incubated and pristine P($PDMS_{11}MA$)$_{38}$-Cl bottlebrushes (Figure 1A and Figure S2B). TGA of P($PDMS_{11}MA$)$_{38}$-Cl followed a two-step mass loss. The first step was within the range of 200−300 °C followed by decomposition of the rest of the sample between 300 and 430 °C. Incubated P($PDMS_{11}MA$)$_{38}$-Cl degraded in one broad transition between 200 and 430 °C. We hypothesize that the decrease in stability after incubation is from an uncatalyzed loss of alkyl halide CEF in a fraction of P($PDMS_{11}MA$)$_{38}$-Cl.

P($PDMS_{11}MA$) was synthesized by free-radical polymerization (RP) (P($PDMS_{11}MA$)-RP) to assess the thermal stability of a bottlebrush lacking alkyl halide CEFs. ^{1}H NMR analysis showed that the mole fraction of vinyl products (f) increased from 3 to 4 mol % after incubation at 170 °C (Figures S6 and S7 and Table 1). The apparent molecular weight and dispersity of P($PDMS_{11}MA$)-RP increased after incubation, and the macromonomer was also visible in the GPC trace. The partial depolymerization of P($PDMS_{11}MA$)-RP at 170 °C may be attributed to bond scission of weak linkages (head−head or unsaturated chain ends) followed by depropagation, similar to poly(methyl methacrylate).[28] TGA analysis showed that the majority of P($PDMS_{11}MA$)-RP degraded between 200 and 350 °C, and the remaining mass loss occurred between 350 and 450 °C. The incubated P($PDMS_{11}MA$)-RP-heat degraded in one broad transition from 200 to 430 °C, similar to P($PDMS_{11}MA$)$_{38}$-Cl-heat.

In summary, the $PDMS_{11}MA$ macromonomer was stable at 170 °C, and the P($PDMS_{11}MA$)-Cl bottlebrush did not depolymerize after incubation without a catalyst. TGA indicated a decrease in P($PDMS_{11}MA$)-Cl thermal stability after incubation. P($PDMS_{11}MA$)$_{38}$-Cl-heat had a comparable trend in mass loss to P($PDMS_{11}MA$)-RP-heat, which suggests uncatalyzed degradation of the alkyl halide during incubation at 170 °C. The P($PDMS_{11}MA$)-RP bottlebrush lacking alkyl halide CEFs partially depolymerized during incubation. The depolymerization of P($PDMS_{11}MA$)-RP was likely triggered by bond scission of weak linkages during incubation, which should be less numerous in a P($PDMS_{11}MA$)$_{38}$-Cl brush prepared by ATRP.

It should be noted that volatiles were not measured during TGA measurements and mass loss may be attributed to

https://doi.org/10.1021/acs.macromol.1c00415
Macromolecules 2021, 54, 5526−5538

Scheme 2. Depolymerization of a P(PDMS$_{11}$MA)$_{38}$-Cl Polymacromonomer in the Presence of CuCl$_2$/TPMA Yields Macromonomer (MM), Oligomeric (Olig), and Bottlebrush (BB) Products

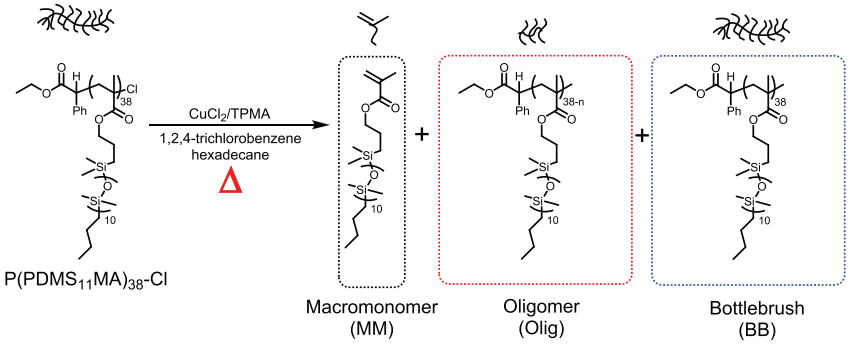

Table 2. Depolymerizations of P(PDMS$_{11}$MA)$_{38}$-Cl[a]

trial	[P(PDMS$_{11}$MA)$_{38}$-Cl]$_0$/[CuCl$_2$]$_0$/[TPMA]$_0$	[P]$_0$ (mM)	time (min)	f (%)[b]	φ_{MM} (%)[c]	φ_{Olig} (%)[c]	φ_{BB} (%)[c]
T1	1/-/-	275	120	1			100
T2	1/0.22/-	275	120	1			100
T3	1/-/0.33	275	120	24	25	7	68
T4	1/0.22/0.22	275	15	8	8	3	89
		275	60	74	76	4	20
		275	75	55	71	8	21
		275	120	79	78	11	11
T5	1/0.22/0.33	275	5	1			100
		275	8	2			100
		275	15	37	30	4	66
		275	60	74	64	6	30
		275	120	75	77	8	15
T6	1/0.22/1.3	275	2	1			100
		275	5	68	41	5	54
		275[d]	10[d]	78[d]	76[d]	6[d]	18[d]
		275	15	77	86	8	6
		275	30	76	83	12	5
		275	60	76	85	10	5
T7	1/0.022/0.13	275	10	60	59	7	34
		275	15	40	35	7	58
		275	60	74	70	10	20
T8	1/0.0038/0.0228	275	60	10			100
		275	120	31	28	4	68
		275	360	42	39	5	56
T9	1/0.22/1.3	138	5	1			100
		138	8	33	30	5	65
		138	15	74	75	5	20
		138	30	66	62	5	33
		138	60	77	79	7	14
T10	1/0.22/1.3	413	1.5	1			100
		413	3	1			100
		413	6.5	1			100
		413	17	1			100
		413	40	31	27	4	69
		413	120	16	15	6	79

[a]Solvent = 1,2,4-trichlorobenzene and 11.7 vol % hexadecane. Total reaction volume = 0.7 mL per entry. Reactions were quenched by injecting ~0.1 mL of a 10 mg/mL SnatchCat stock solution in 1,2,4-trichlorobenzene immediately followed by a blanket of air over the open flask. [b]The mole fraction of vinyl-terminated products determined by ^{1}H NMR of the crude reaction mixture. [c]The weight fraction of the polymeric fraction determined by peak fitting of GPC traces using Origin software. Peak fits are provided in the Supporting Information. [d]Volume = 2 mL.

decomposition of the end groups, the methacrylate backbone, or the PDMS side chain; however, it is more likely that mass loss at low temperature closely follows decomposition of the chain end due to the high thermal stability of PDMS.[52,53] Thermal degradation of P(PDMS$_{11}$MA)-Cl could be compared to previous studies on halogen-capped polymethacrylates. Less mass loss was observed in TGA of bromine-capped PMMA-Br between 160 and 250 °C, relative to PMMA prepared by RP.[54,55] However, elimination and lactonization of the chain end were observed after isothermal incubation of PMMA-Br and

https://doi.org/10.1021/acs.macromol.1c00415
Macromolecules 2021, 54, 5526−5538

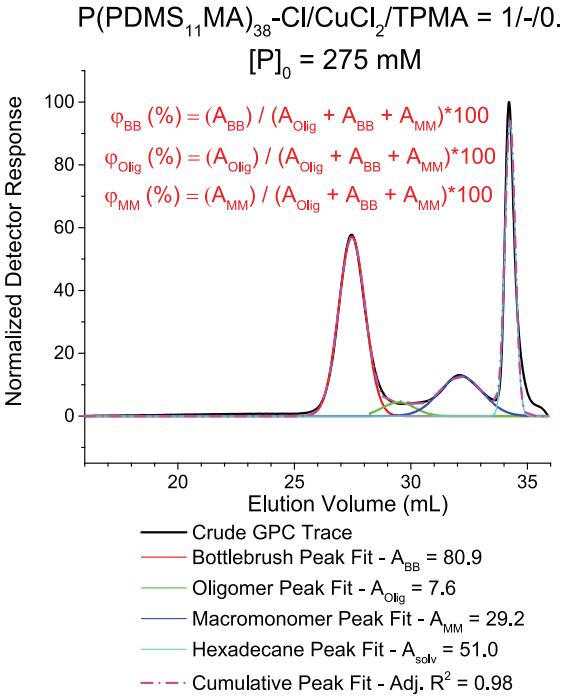

Figure 2. Characterization of GPC traces after depolymerization in trial **T3** by peak fitting to the bottlebrush (BB), oligomer (Olig), macromonomer (MM), and solvent (solv) in units of elution volume vs normalized refractive index detector response. The peak areas of the bottlebrush (A_{BB}), oligomers (A_{Olig}), macromonomer (A_{MM}), and solvent (A_{solv}) were obtained by multiple peak fitting to the respective peaks in the crude GPC trace. The weight fractions of the bottlebrush (φ_{BB}), oligomers (φ_{Olig}), and macromonomer (φ_{MM}) are given by the ratio of the peak area to the sum of all polymeric peak areas times 100. Conditions: $[P(PDMSMA)_{38}\text{-}Cl]_0/[CuCl_2]_0/[TPMA]_0$ = 1/-/0.33, $[P]_0$ = 275 mM, T = 170 °C, and solvent = 11.7 vol % hexadecane and 1,2,4-trichlorobenzene.

PMMA-Cl at 150 °C by NMR and MALDI-TOF in several publications.[56−58] Incubation increased the thermal stability of bromine-capped poly(methyl methacrylate), poly(ethyl methacrylate), poly(*n*-butyl methacrylate), and poly(*n*-hexyl methacrylate) prepared by ATRP using a 2,2,2-tribromoethanol initiator.[56] Uncatalyzed degradation of the chain end will affect the thermal stability of polymers prepared by ATRP and needs to be understood in the context of depolymerizations and applications. We are currently investigating this topic in greater detail.

Catalyzed Depolymerizations. Catalyzed depolymerizations were conducted with a typical $CuCl_2$/TPMA ATRP catalyst in a 1,2,4-trichlorobenzene/hexadecane cosolvent system (Scheme 2). The $CuCl_2$/TPMA catalyst is sparingly soluble in 1,2,4-trichlorobenzene, but nonpolar P-$(PDMS_{11}MA)_{38}$-Cl is insoluble in polar 1,2,4-trichlorobenzene. Hexadecane (11.7 vol %) was added to dissolve the bottlebrush. The concentration of P$(PDMS_{11}MA)_{38}$-Cl is given as $[P]_0$ and is analogous to $[M]_0$, so $[P]_0$ = 275 mM corresponds to a 275 mM concentration of $PDMS_{11}MA$ repeat units and an alkyl halide concentration of 7.2 mM. For every set of conditions in Table 2, depolymerizations were repeated and stopped at different times, corresponding to each reported time point. Results are in the format **Trial-Time** (i.e., **T4-60** is a depolymerization with conditions **T4** conducted for 60 min). Experiments were conducted in 10 mL Schlenk flasks with total reaction volumes

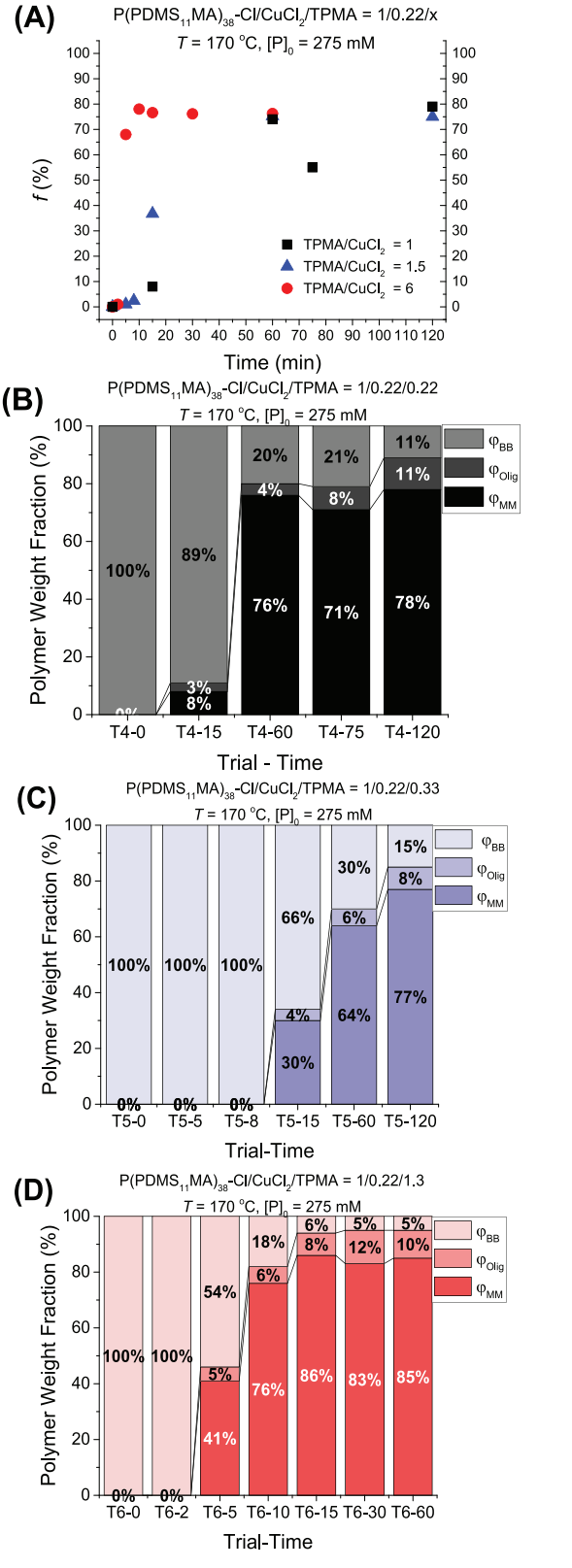

Figure 3. Yield of P$(PDMS_{11}MA)_{38}$-Cl depolymerizations at $[TPMA]_0/[CuCl_2]_0$ = 1, 1.5, and 6 (**T4−T6** in Table 2). (A) Mole fraction of recovered vinyl products (f) for trials **T4−T6**. The weight fractions of polymer species separated by φ_{MM}, φ_{Olig}, and φ_{BB} are given for trials (B) **T4**, (C) **T5**, and (D) **T6**. Conditions: $[P(PDMSMA)_{38}\text{-}Cl]_0/[CuCl_2]_0/[TPMA]_0$ = 1/0.22/X with X = 0.22, 0.33, and 1.3. Temperature = 170 °C. $[P]_0$ = 275 mM in 1,2,4-trichlorobenzene and 11.7 vol % hexadecane.

https://doi.org/10.1021/acs.macromol.1c00415
Macromolecules 2021, 54, 5526−5538

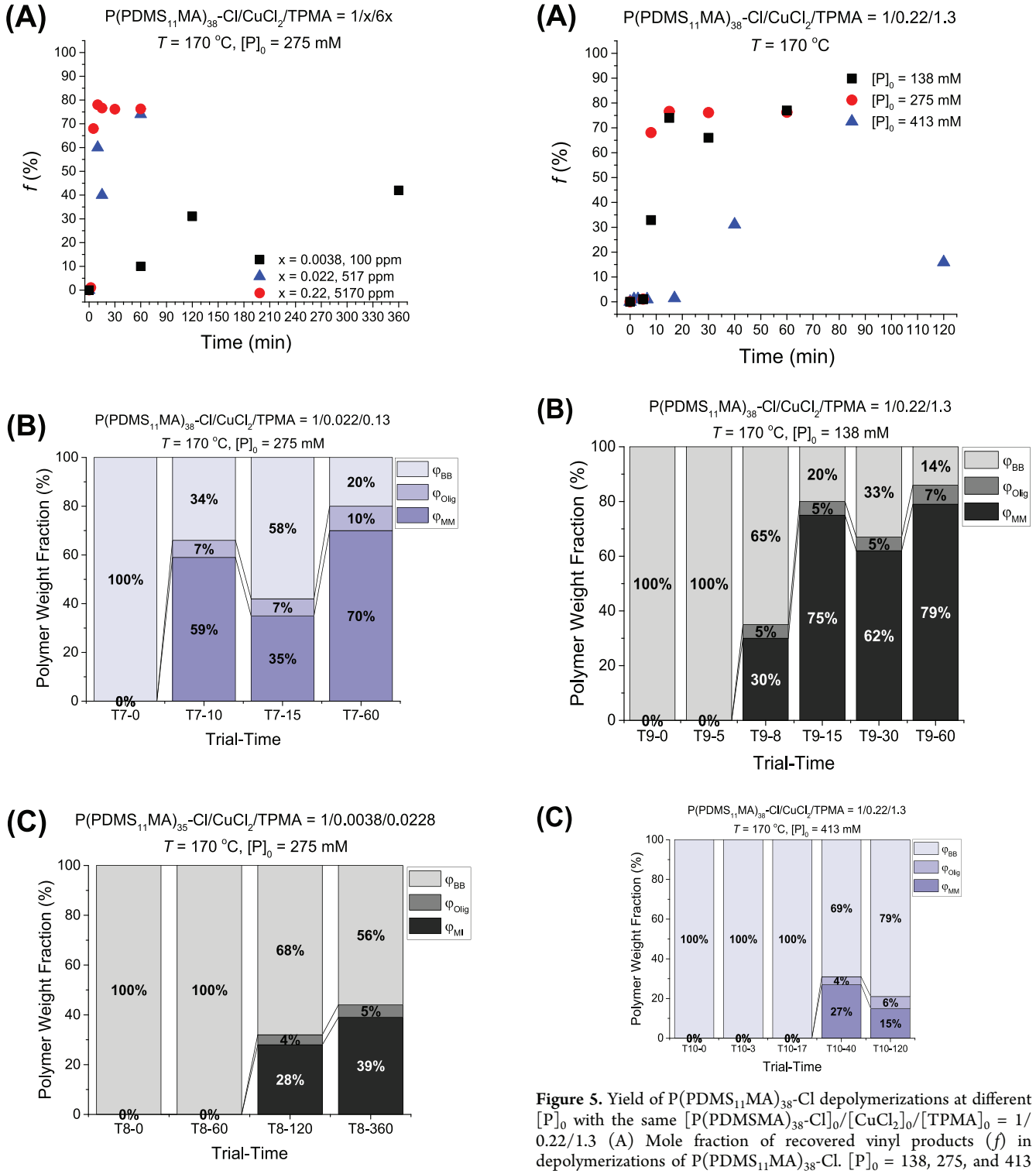

Figure 4. Yield of $P(PDMS_{11}MA)_{38}$-Cl depolymerizations with $[TPMA]_0/[CuCl_2]_0 = 6$ at 5170 ppm (**T6**), 517 ppm (**T7**), and 100 ppm (**T8**) conducted for different amounts of time (Table 2). (A) Mole fraction of recovered vinyl products (f). The weight fractions of polymer species separated by φ_{MM}, φ_{Olig}, and φ_{BB} for recipe are given in (B) **T7** and (C) **T8**. Conditions: $[P(PDMSMA)_{38}\text{-Cl}]_0/[CuCl_2]_0/[TPMA]_0 = 1/X/6X$ with $X = 0.22$, 0.022, and 0.0038. Temperature = 170 °C. $[P]_0$ = 275 mM in 1,2,4-trichlorobenzene and 11.7 vol % hexadecane.

Figure 5. Yield of $P(PDMS_{11}MA)_{38}$-Cl depolymerizations at different $[P]_0$ with the same $[P(PDMSMA)_{38}\text{-Cl}]_0/[CuCl_2]_0/[TPMA]_0 = 1/0.22/1.3$ (A) Mole fraction of recovered vinyl products (f) in depolymerizations of $P(PDMS_{11}MA)_{38}$-Cl. $[P]_0$ = 138, 275, and 413 mM in **T9**, **T6**, and **T10**, respectively. The weight fractions of polymer species separated by φ_{MM}, φ_{Olig}, and φ_{BB} are given in (B) **T9** and (C) **T10**. Temperature = 170 °C. The volume fraction of hexadecane was kept constant at 11.7 vol %, and the volume fraction of 1,2,4-trichlorobenzene was scaled with repeat unit concentration.

of 0.7 mL. They were stopped by opening the flask and then adding ~0.1 mL of a 10 mg/mL 1,4-bis(3-isocyanopropyl)-piperazine (SnatchCat) stock solution in 1,2,4-trichlorobenzene to quench the active CuCl/TPMA catalyst followed by a blanket of air over the hot open flask. The SnatchCat ligand quenches ATRP by strongly and irreversibly binding to Cu(I).[59] Air oxidizes the residual CuCl/TPMA activator and acts as an inhibitor for radical polymerization.[60]

https://doi.org/10.1021/acs.macromol.1c00415
Macromolecules 2021, 54, 5526−5538

Table 3. Observed Rate Constants of $CuCl_2$/L Reduction ($k_{red,obs}$) with L = TPMA or TPMA*[3] from 130 to 170 °C

$[L]_0/[CuCl_2]_0$	L	temperature (°C)	$k_{red,obs} \times 10^4$ (s^{-1})[a]
1	TPMA	170	3.02 ± 0.10
1.5	TPMA	170	3.35 ± 0.17
6	TPMA	170	17.7 ± 0.94
6	TPMA	150	2.45 ± 0.12
6	TPMA	130	
6	TPMA*[3]	170	6.68 ± 0.56

[a]Taken as the slope of the first-order kinetic plots in Figure 6. The margin of error is given as the 95% confidence interval after linear fitting of experimental data with a set *y*-intercept = 0. $[CuCl_2]_0$ = 1.24 mM, and $[L]_0$ is scaled to $[CuCl_2]_0$. Solvent = 18/82 v/v% DMF/1,2,4-trichlorobenzene.

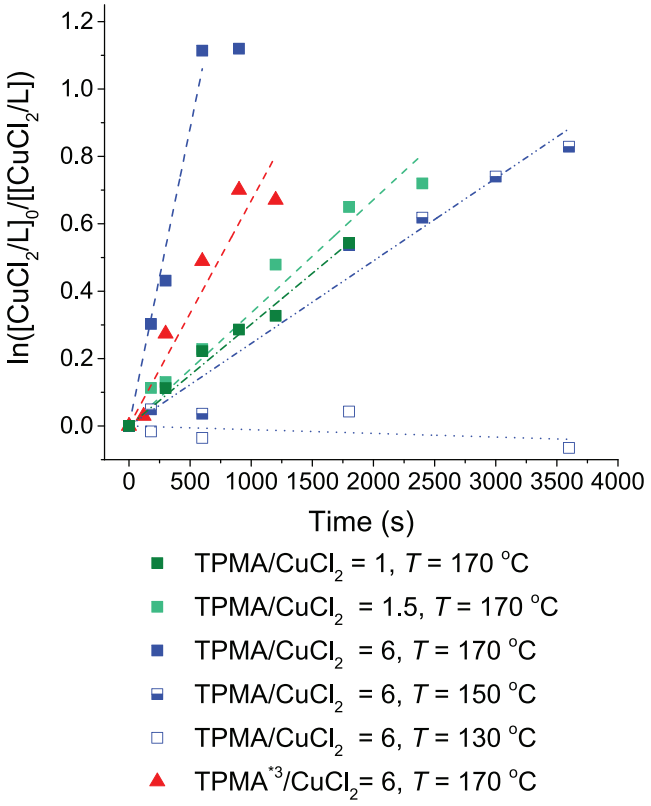

Figure 6. First-order kinetic plot of $[CuCl_2]/[L]$ reduction with $[L]/[CuCl_2]$ = 1 to 6, *T* = 130−170 °C, and L = TPMA or TPMA*[3]. Conditions: $[CuCl_2]_0$ = 1.24 mM, and $[L]_0$ is scaled to $[CuCl_2]_0$. Solvent = 18/82 v/v% DMF/1,2,4-trichlorobenzene. Reduction experiments were collected by UV/Vis using a Schlenk-modified cuvette. Absorbance was recorded after 1 min of cooling to avoid melting the equipment.

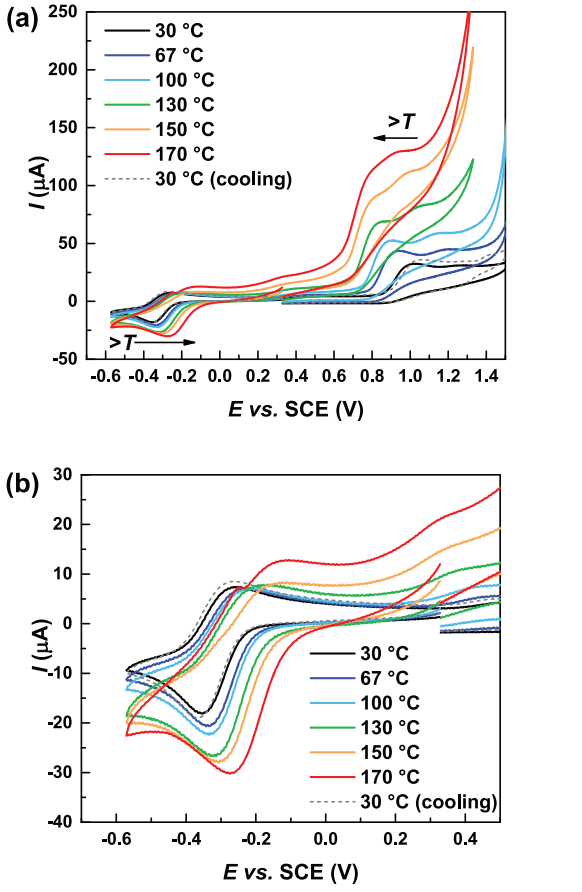

Figure 7. CVs of 1.2 mM $CuCl_2$/TPMA in DMF + 0.1 M Et_4NBF_4 (a) and zoomed-in image of the same CVs (b), recorded at increasing temperature, on a GC working electrode at ν = 0.2 V s^{-1}, using a silver wire as a quasi-reference electrode and converted to SCE by adding ferrocene as an internal standard.

The weight fractions of the bottlebrush (φ_{BB}), oligomers (φ_{Olig}), and macromonomer (φ_{MM}) were determined by multiple peak fitting of the refractive index signal relative to the elution volume in the crude THF GPC traces with Origin software (Figure 2).[61] Peak fitting was generally conducted by fitting to the bottlebrush, oligomer, macromonomer, and solvent peaks. This procedure is discussed in detail in the Supporting Information. The peak areas of the bottlebrush (A_{BB}), oligomers (A_{Olig}), macromonomer (A_{MM}), and solvent (A_{solv}) were obtained once the multiple peak fit closely matched the crude GPC trace with an $R^2 > 0.97$ (Figure 2). φ_{MM}, φ_{Olig}, and φ_{BB} are defined as the ratio of their respective peak area to the sum of all polymer peak areas (Figure 2).

No depolymerization was observed when $P(PDMS_{11}MA)_{38}$-Cl was diluted to $[P]_0$ = 275 mM at 170 °C (Table 2, **T1**), as well as upon addition of $CuCl_2$, because bare $CuCl_2$ acts as an inhibitor for radical polymerization (Table 2, **T2**).[62] Addition of 0.3 equiv of TPMA relative to the alkyl halide, in the absence of $CuCl_2$, gave *f* = 24% (Table 2, **T3**). Initiation could occur by charge transfer between TPMA and alkyl halide CEFs to yield the chain-end radical, TPMA radical cation, and Cl^-. This reaction was reported to have a small contribution to activator regeneration in photoATRP at ambient temperature but could be more significant at higher temperatures.[63]

Addition of both $CuCl_2$ and TPMA at $[P(PDMS_{11}MA)_{38}\text{-}Cl]_0/[CuCl_2]_0/[TPMA]_0$ = 1/0.22/0.22 recovered [*f*, φ_{MM}] = [79%, 78%]. (**T4-120**, Table 2). The higher yield is attributed to activation and delayed termination by an ATRP process regulated by the $CuCl_2$/TPMA catalyst. Activation leads to depolymerization because the reaction temperature was at elevated temperature in the absence of the $PDMS_{11}MA$ macromonomer. Depolymerizations were accelerated by increasing $[TPMA]_0/[CuCl_2]_0$ from 1 to 1.5 and 6 in trials **T5** and **T6**, respectively (Table 2). **T4-15** recovered [*f*, φ_{MM}] = [8%, 8%]. Meanwhile, **T5-15** reached [*f*, φ_{MM}] = [37%, 30%], and **T6-15** recovered [*f*, φ_{MM}] = [77%, 86%]. The increase in depolymerization rate with equivalents of TPMA was attributed

https://doi.org/10.1021/acs.macromol.1c00415
Macromolecules 2021, 54, 5526−5538

Table 4. Depolymerization/Repolymerization of $P(PDMS_{11}MA)_{38}$-Cl[a]

cycle	step in the cycle	additive − equivalents rel. to $[P(PDMS_{11}MA)_{38}\text{-Cl}]_0$	cumulative reaction time (hh:mm)	temp. (°C)	f[b] (%)	φ_{MM}[c] (%)	φ_{Olig}[c] (%)	φ_{BB}[c] (%)
C1	D1[d]		00:10	170	78	76	6	18
	P1		19:10	22	71	70	10	20
	D2		19:30	170	75	76	9	15
C2[e]	D1		00:10	170	81	82	7	11
	P1	AIBN − 0.4 equiv	22:10	22	65	64	18	18
			46:10	22	40	37	10	53
			72:10	22	4	9	8	83
	D2		72:40	170	42	39	13	48
C3[f]	D1		00:15	170	79	76	8	16
	P1	EClPA − 0.36 equiv	70:15	22	5	5	15	80
	D2		70:45	170	39	31	23	46
	P2	EClPA − 0.36 equiv	140:45	22	10	17	18	65
	D3		141:15	170	18	34	9	57
	P3	EClPA − 0.36 equiv	211:15	22	3	19	13	68
	D4		211:45	170	6	17	13	70

[a]Conditions: $[P(PDMS_{11}MA)_{38}\text{-Cl}]_0/[CuCl_2]_0/[TPMA]_0$ = 1/0.22/1.3 in D1 for all cycling experiments. Additives added at the start of P1 are stated relative to the initial molar equivalents of the $P(PDMS_{11}MA)_{38}$-Cl alkyl halide. The solvent was 1,2,4-trichlorobenzene with a constant 11.7% volume of hexadecane. Total reaction volume = 2 mL. [b]The fraction of vinyl products by ^{1}H NMR of the crude reaction mixture. [c]The weight fraction of the polymeric fraction determined by peak fitting of GPC traces using Origin software. [d]The same run as **T6−10**. [e]Hexadecane (6 vol %) was used. [f]The ligand is BPMODA*.

Scheme 3. Schematic of Depolymerization/Repolymerization Cycling Experiments

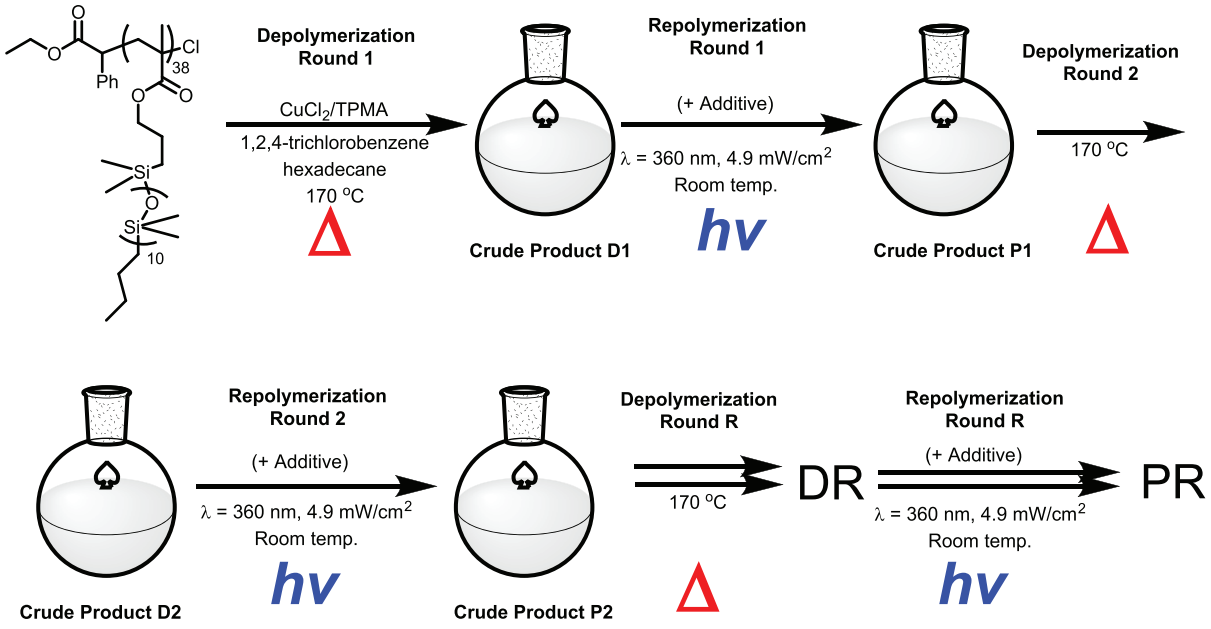

to reduction of $CuCl_2$/TPMA by electron transfer from the excess ligand, similar to previously reported ARGET polymerizations of methacrylates.[64,65] Faster reduction of the catalyst accelerated the ATRP reactions. Trials **T4−T6** stopped at approximately the same f of ∼80% when conducted for longer reaction times, despite the differences in depolymerization rates (Figure 3).

Independent analysis of φ_{MM}, φ_{Olig}, and φ_{BB} provided insight into the product distributions of depolymerization reactions (Figure 3). φ_{BB} decreased with reaction time until it plateaued once no further depolymerization was observed. The φ_{Olig} and φ_{MM} concurrently increased as φ_{BB} decreased until they reached their own respective plateaus.

The selectivity of **T4−T6** was assessed by comparison of φ_{MM}, φ_{Olig}, and φ_{BB}. The macromonomer yield improved for depolymerizations with excess TPMA, with φ_{MM} = 78, 77, and 85% for **T4-120**, **T5-120**, and **T6-60**, respectively. φ_{MM} was generally higher than f = 79, 75, and 76% for the same reactions, which may be due to a loss of vinyl functionalities in a fraction of unimers by termination. There was more variance between φ_{Olig} and φ_{BB}. **T5-120** had the most unreacted bottlebrush, with $[\varphi_{BB}, \varphi_{Olig}]$ = [15%, 8%]. The selectivity was improved in **T4-120** to $[\varphi_{BB}, \varphi_{Olig}]$ = [11%, 11%]. **T6-60** was the most selective, with $[\varphi_{BB}, \varphi_{Olig}]$ = [5%, 10%]. Thus, the highest $[TPMA]_0/[CuCl_2]_0$ gave the fastest and most selective depolymerization.

$CuCl_2$ concentration was lowered from 5170 ppm (**T6**) to 517 ppm (**T7**) and 100 ppm (**T8**) at a constant $[TPMA]_0/[CuCl_2]_0$ = 6 to determine the effect of catalyst loading. Lower catalyst loadings decreased the rate of depolymerization (Figure 4). **T7-60** reached $[f, \varphi_{MM}]$ = [74%, 70%], while **T8-60**

https://doi.org/10.1021/acs.macromol.1c00415
Macromolecules 2021, 54, 5526−5538

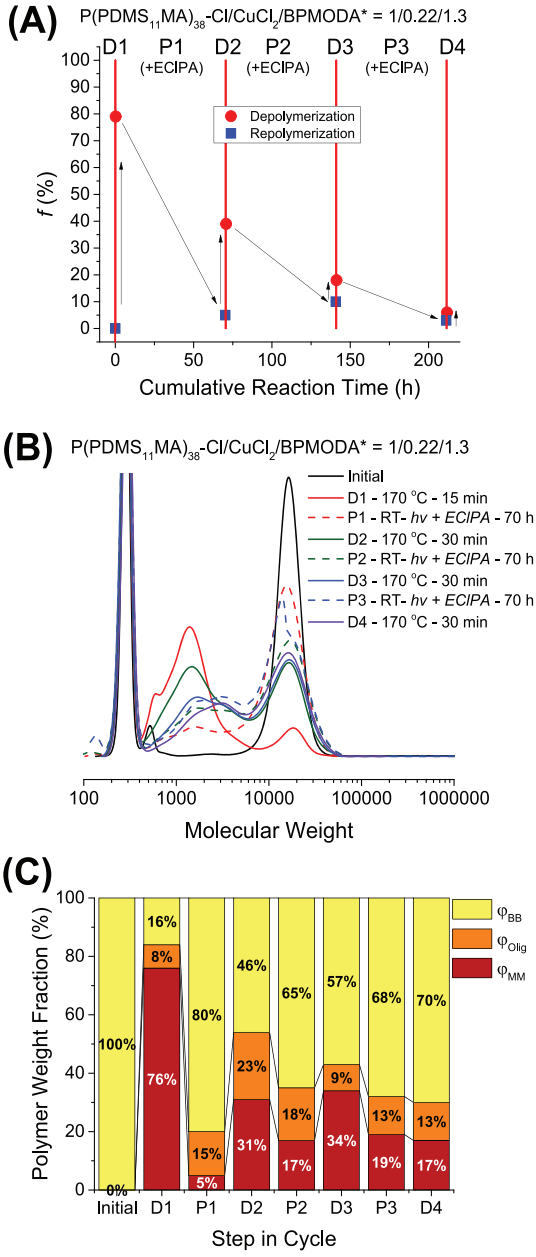

Figure 8. (A) Kinetic trace of the C3 cycling experiment with the addition of the EClPA initiator in each repolymerization step in the cycle. Vertical red lines correspond to the start and end of a step in the cycle. The black arrows are a guide for the eyes. (B) Crude GPC traces taken at the end of each step of cycling experiment C3. The trace is normalized to the height of the solvent peak and cut off at the height of the initial P(PDMS$_{11}$MA)$_{38}$-Cl peak. (C) Bar graph of polymer weight fractions in each cycling step. Conditions are given in Table 4.

recovered f = 10%. **T8-360** recovered [f, φ_{MM}] = [42%, 39%]. The selectivity was compared between trials **T6-5**, **T7-15**, and **T8-360** because the three trials stopped at φ_{BB} of ∼55%. **T6-5** recovered [φ_{MM}, φ_{Olig}, φ_{BB}] = [41%, 5%, 54%] and had the highest weight fraction of oligomers in this set. Decreasing catalyst loading to 517 ppm slowed depolymerization and increased φ_{Olig} to 7% (**T7-15**). **T8-360** had comparable selectivity, with [φ_{MM}, φ_{Olig}, φ_{BB}] = [39%, 5%, 56%], at the cost of a much slower depolymerization.

Depolymerizations were attempted by ATRP with [P(PDMSMA)$_{38}$-Cl]$_0$/[CuCl$_2$]$_0$/[TPMA]$_0$ = 1/0.22/1.3 scaled

Scheme 4. Proposed Mechanism of Depolymerizations by ATRP with Activator Regeneration at High Temperature

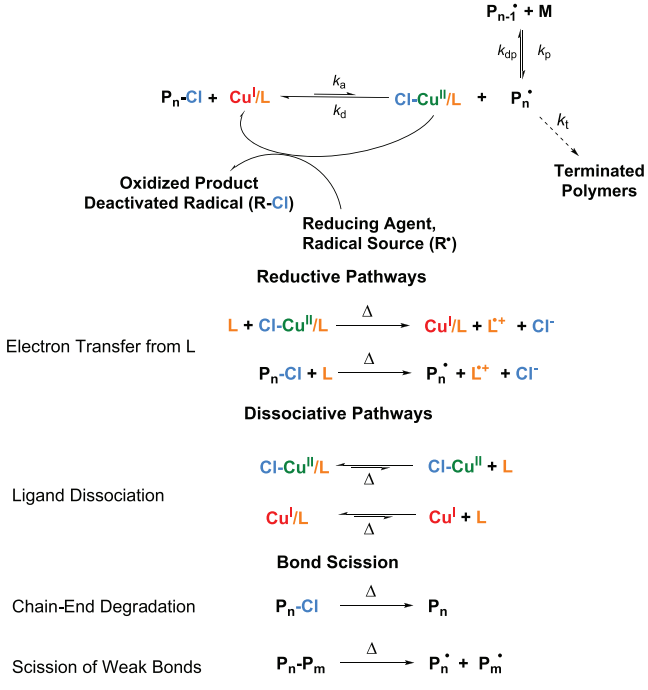

to [P]$_0$ = 138 mM (**T9**) and 413 mM (**T10**) at a constant 11.7% volume of hexadecane. The depolymerizations conducted at [P]$_0$ = 413 mM (**T10**) were slower than the more dilute depolymerizations (Figure 5). Reaction **T9** with [P]$_0$ = 138 mM proceeded at a comparable rate to the depolymerization **T6** with slightly lower selectivity to the macromonomer (Figure 5 and Figure S15).

Summary. Depolymerizations of a chlorine-capped P(PDMS$_{11}$MA)$_{38}$-Cl were conducted at 170 °C. **T1** and **T2** confirmed that no depolymerization occurred within 2 h in the absence of TPMA. Addition of TPMA in **T3** induced depolymerization by activation of alkyl halide CEFs via charge transfer.[63] Depolymerization occurred because the reaction mixture was at high temperature, near or above the T_c, in the absence of the PDMS$_{11}$MA macromonomer.

Depolymerizations with CuCl$_2$ and TPMA at a 5170 ppm catalyst loading recovered macromonomers with f of ∼80% in **T4**−**T6**. The increase in yield relative to **T1**−**T3** was attributed to activation and reduced termination by an ATRP process regulated by the CuCl$_2$/TPMA catalyst. The rate, yield, and selectivity of depolymerizations improved by increasing [TPMA]$_0$/[CuCl$_2$]$_0$ from 1 to 6. Lower catalyst loadings improved selectivity toward the macromonomer at the expense of a much slower depolymerization (Table 2, **T8**). Depolymerization at [P]$_0$ = 138 mM (**T9**) was comparable to the analogous depolymerization at a higher [P]$_0$ = 275 mM, but depolymerization at [P]$_0$ = 413 mM (**T10**) was significantly slower than the more dilute reactions.

The differences in the yield, selectivity, and reaction rate with catalyst and ligand concentrations prompted us to characterize the stability and reactivity of the CuCl$_2$/TPMA catalyst with the TPMA ligand at high temperature.

Catalyst Characterization. Reduction experiments were conducted to clarify the effects of CuCl$_2$/L stoichiometry and catalyst activity at high temperature. The reduction of CuCl$_2$ with TPMA and tris(3,5-dimethyl-4-methoxy-2-pyridylmethyl)-

https://doi.org/10.1021/acs.macromol.1c00415
Macromolecules 2021, 54, 5526−5538

amine (TPMA*^{3}) ligands was monitored as a decrease in the absorbance at 960 and 940 nm, respectively, via UV/Vis spectroscopy. DMF (18 vol %) was added to all reduction experiments listed in Table 3 to improve the solubility of the complexes. The observed rate constants of $CuCl_2$/TPMA and $CuCl_2$/TPMA*^{3} reduction ($k_{red,obs}$) are given as the slope of the first-order kinetic plot for reduction defined by the decrease in absorbance at 960 and 940 nm, respectively. Time is given as the amount of time spent inside the hot oil bath; however, all spectra were recorded after 1 min of cooling to avoid damage to the UV/Vis cell.

$CuCl_2$/TPMA complexes with 6 equiv of the ligand had no observable reduction at 130 °C after 1 h (Figure 6 and Figure S18). An increase in temperature to 150 °C led to slow reduction at $k_{red,obs} = 2.45 \times 10^{-4}$ s^{-1}. Further increasing temperature to 170 °C led to a 7 times higher $k_{red,obs} = 17.70 \times 10^{-4}$ s^{-1}, i.e., 7 times higher than at T = 150 °C.

$CuCl_2$ was stirred at 170 °C with a decreasing amount of TPMA. Equimolar $[TPMA]_0/[CuCl_2]_0 = 1$ showed a decrease in absorbance at 960 nm, indicating reduction of $CuCl_2$. A slight excess of the TPMA ligand at $[TPMA]_0/[CuCl_2]_0 = 1.5$ led to a slightly higher $k_{red,obs} = 3.35 \times 10^{-4}$ s^{-1}, which was still 5.3 times smaller than $[TPMA]_0/[CuCl_2]_0 = 6$ at the same temperature. The $CuCl_2$/TPMA catalyst was left open to air after heating for 15 min at 170 °C to qualitatively determine if the catalyst cycle was reversible. After 2 min, there was an increase in $CuCl_2$/TPMA absorption at 960 nm in the UV/Vis trace (Figure S18). The solution was less transparent after oxidation of the flask, likely due to partial evaporation of DMF from the open flask diminishing the catalyst solubility.

The absorbance of $[TPMA^{*3}]_0/[CuCl_2]_0 = 6$ was tracked over time to determine the effect of catalyst activity on thermal reduction at 170 °C. $CuCl_2$/TPMA*^{3} has more negative reduction potential than $CuCl_2$/TPMA, thus exhibiting higher ATRP activity and slower reduction, with $k_{red,obs}$ of 6.68×10^{-4} s^{-1}.[61,66]

The reversibility of the $CuCl_2$/TPMA redox cycle was assessed by cyclic voltammetry (CV) at increasing temperature in 1,2,4-trichlorobenzene with 18 vol % DMF and 0.1 M Et_4NBF_4 as a supporting electrolyte. CVs showed a quasi-reversible redox couple as the temperature was increased from 25 to 170 °C (Figure S20). The current intensity of both cathodic and anodic peaks increased with temperature up to 100 °C due to an increase in the diffusion coefficients of both Cu(II) and Cu(I) species. The decrease in current intensity observed at T > 100 °C could indicate changes in the catalyst speciation. Increasingly positive current was recorded at potentials slightly more positive than the catalyst reduction, plausibly due to oxidation of Cl^-; however, the narrow electrochemical window of 1,2,4-trichlorobenzene hindered further analysis.

Therefore, CV of $CuCl_2$/TPMA was conducted in pure DMF with a 0.1 M Et_4NBF_4 supporting electrolyte. The larger electrochemical window of DMF allowed for investigation within a wider range of potentials. The CVs showed reversible reduction and oxidation of the catalyst for T within 30−170 °C (Figure 7). The current intensity of the catalyst redox signals increased with temperature, while the potential progressively shifted to more positive values with increasing T.[67] The oxidation of Cl^- at E of ∼1 V vs SCE shifted toward more negative potentials with increasing T. Upon lowering the temperature from 170 to 30 °C, the recorded signal was nearly identical to the initial scan at 30 °C, suggesting that $CuCl_2$/TPMA is stable at high temperature.

Depolymerization/Repolymerization Cycling. Cycling experiments were conducted with alternating rounds of depolymerization at 170 °C and repolymerization by photoATRP at room temperature. PhotoATRP regenerates the majority of the Cu(I) activator through a photoinduced electron transfer process between the excited X-Cu(II)/L catalyst and excess alkylamines at ambient temperature.[63] Thus, photoATRP does not require additional additives, and an analogous recipe to depolymerizations could be employed. The cycling experiments used the same conditions as **T6**, with 5170 ppm of the copper catalyst and $[TPMA]_0/[CuCl_2]_0 = 6$ (Table 4). Each round consisted of one depolymerization (DR) followed by polymerization of the crude product from the first step without purification (PR) and so on. The postscript -R denotes the round number (Scheme 3).

Depolymerization C1-D1 recovered f = 78% in 10 min. Repolymerization C1-P1 polymerized 7% monomer in 19 h (Table 4 and Figure S21). The second depolymerization C1-D2 recovered a portion of the repolymerized product. The slow rate of polymerization is attributed to a loss of most of the alkyl halide functionalities after the first depolymerization and slow precipitation of the catalyst from the nonpolar mixture.

In cycling experiment C2, the volume fraction of hexadecane was reduced from 11.7 to 6 vol % to improve the solubility of the copper catalyst at the expense of polymer solubility (Figure S24). C2-D1 recovered f = 81% (Table 4 and Figure S22). Repolymerization C2-P1 reached f = 4% in 72 h by a photoinduced reverse ATRP with $CuCl_2$/TPMA reduction by the photoATRP process and azobisisobutyronitrile (AIBN) decomposition under UV light. The flask was transferred to a hot oil bath set to 170 °C without purification for cycle C2-D2, where f = 42% was recovered in 30 min.

Multiple cycles were attempted with a $CuCl_2$/bis[2-(4-methoxy-3,5-dimethyl)pyridylmethyl]octadecylamine ($CuCl_2$/BPMODA*) catalyst, which has comparable activity to TPMA but is highly soluble in nonpolar solvents.[68] C3-D1 reached f = 81% in 15 min (Table 4 and Figure 8). Repolymerization C3-P1 was started upon photoirradiation with an additional 0.36 equiv of the EClPA initiator. The majority of the macromonomer polymerized over 70 h (f = 5%, Table 4). C3-D2 isolated approximately half of the macromonomer compared to the first cycle (f = 39%, Table 4). The macromonomer remaining after depolymerization C3-D2 was repolymerized for a second time in C3-P2 then depolymerized to a lower yield (f = 18%) in C3-D3. The remaining 18% macromonomer was repolymerized again (C3-P3) then depolymerized to yield only f = 6% in the last C3-D4 depolymerization. The decrease in macromonomer recovery with each consecutive depolymerization cycle confirmed a loss in chain-end functionalities during both depolymerization and repolymerization reactions. Chains lacking the alkyl halide cannot be activated by the catalyst in a depolymerization or polymerization by ATRP. A fraction of chains terminates, or degrades, with each step in the cycle. Accumulation of nonfunctional chains reduces the macromonomer available for polymerization and the macroinitiator available for depolymerization.

Mechanistic Discussion. Thermal stability control experiments confirmed that the $PDMS_{11}MA$ macromonomer was stable at 170 °C and depolymerization of the P($PDMS_{11}MA$)-Cl bottlebrush did not occur without a catalyst at 170 °C. The P($PDMS_{11}MA$)-RP bottlebrush partially depolymerized after incubation due to a presumed larger number of weak links in the polymer backbone. TGA indicated a decrease in P-

https://doi.org/10.1021/acs.macromol.1c00415
Macromolecules 2021, 54, 5526−5538

($PDMS_{11}MA$)-Cl thermal stability after incubation, such that the trend in $P(PDMS_{11}MA)_{38}$-Cl-heat mass loss was comparable to $P(PDMS_{11}MA)$-RP-heat. Thus, scission of weak links may induce depolymerization at 170 °C, and uncatalyzed degradation can reduce the stability of macroinitiators prepared by ATRP. The proposed mechanism for a catalyzed depolymerization by atom transfer radical polymerization at high temperature is given in Scheme 4.

The catalyzed depolymerizations in Table 2 were conducted at high temperature in the absence of the macromonomer. Since T was kept constant, the differences in the yield, selectivity, and depolymerization rate depended on the rate of atom transfer with the alkyl halide CEF for depolymerizations at the same $[P]_0$ = 275 mM.

Activator regeneration of Cu(I) was promoted by the TPMA ligand acting as the reducing agent in an ARGET process.[64,65] UV/Vis reduction experiments showed that $k_{red,obs}$ increased ~5 times upon increasing $[TPMA]/[CuCl_2]$ from 1.5 to 6, in agreement with the observed increase in the depolymerization rate under similar conditions. The reduction experiment and depolymerization performed at $[TPMA]/[CuCl_2]$ = 1 showed that Cu(II) reduction and depolymerization initiation could occur in the absence of an excess ligand. This behavior could be explained by considering dissociation of the ligand from the copper complex, generating a free ligand that could reduce $CuCl_2$/TPMA and/or $CuCl_2$ species. Most of the catalysts remained active and stable, as evidenced by the reversible cyclic voltammograms obtained at 170 °C. TPMA could also activate the alkyl halide via charge transfer, similar to a photoATRP at ambient temperature.[63]

CONCLUSIONS

Depolymerization of a methacrylic $P(PDMS_{11}MA)_{38}$-Cl bottlebrush was catalyzed by Cu(II) complexes with activator regeneration at 170 °C. Efficient atom transfer between the alkyl halide CEF and the catalyst enabled 80% monomer recovery within short reaction times. The rate and control over depolymerizations were improved by activator regeneration from the TPMA ligand. Depolymerization yield and selectivity were improved by increasing equivalents of the TPMA ligand at higher catalyst loadings. Decreasing catalyst loadings from 5170 to 517 and 100 ppm gave slightly better selectivity toward the macromonomer over oligomers but significantly slower depolymerizations. Depolymerizations by ATRP at a higher initial polymer concentration were slower than at higher dilutions.

The $CuCl_2$/TPMA catalyst could be progressively reduced through electron transfer reactions from the TPMA ligand in an ARGET process. The catalyst could also be reduced through other radical-creating pathways.

Further progress in this area can be reached through fundamental studies of catalysts and polymers at high temperatures. Retention of chain-end functionalities at elevated temperature is of particular importance.

ASSOCIATED CONTENT

Supporting Information

The Supporting Information is available free of charge at https://pubs.acs.org/doi/10.1021/acs.macromol.1c00415.

Materials and instrumentation, synthetic procedures, ^1H NMR spectra, select crude ^1H NMR spectra, first derivative TGA curves, GPC traces and curve fitting analysis, UV/Vis, and cyclic voltammetry measurements (PDF)

AUTHOR INFORMATION

Corresponding Author

Krzysztof Matyjaszewski − *Department of Chemistry, Center for Macromolecular Engineering, Carnegie Mellon University, Pittsburgh, Pennsylvania 15213, United States;* orcid.org/0000-0003-1960-3402; Email: matyjaszewski@cmu.edu

Authors

Michael R. Martinez − *Department of Chemistry, Center for Macromolecular Engineering, Carnegie Mellon University, Pittsburgh, Pennsylvania 15213, United States;* orcid.org/0000-0002-6211-763X

Sajjad Dadashi-Silab − *Department of Chemistry, Center for Macromolecular Engineering, Carnegie Mellon University, Pittsburgh, Pennsylvania 15213, United States;* orcid.org/0000-0002-4285-5846

Francesca Lorandi − *Department of Chemistry, Center for Macromolecular Engineering, Carnegie Mellon University, Pittsburgh, Pennsylvania 15213, United States;* orcid.org/0000-0001-5253-8468

Yuqi Zhao − *Department of Materials Science and Engineering, Carnegie Mellon University, Pittsburgh, Pennsylvania 15213, United States;* orcid.org/0000-0002-4438-3635

Complete contact information is available at: https://pubs.acs.org/10.1021/acs.macromol.1c00415

Notes

The authors declare no competing financial interest.

ACKNOWLEDGMENTS

We would like to acknowledge financial support from NSF DMR 1921858 and NSF DMR 1501324. The NMR instrumentation at the Carnegie Mellon University was partially supported by the NSF (CHE-0130903, CHE-1039870, and CHE-1726525).

REFERENCES

(1) Geyer, R.; Jambeck, J. R.; Law, K. L. Production, use, and fate of all plastics ever made. *Science* **2017**, *3*, e1700782.

(2) Hong, M.; Chen, E. Y.-X. Chemically recyclable polymers: a circular economy approach to sustainability. *Green Chem.* **2017**, *19*, 3692−3706.

(3) *Mechanical Recycling, Plastic Recyclers Europe.* http://www.plasticsrecyclers.eu/mechanical-recycling.

(4) Coates, G. W.; Getzler, Y. D. Y. L. Chemical recycling to monomer for an ideal, circular polymer economy. *Nat. Rev. Mater.* **2020**, *5*, 501−516.

(5) Phillips, S. T.; DiLauro, A. M. Continuous Head-to-Tail Depolymerization: An Emerging Concept for Imparting Amplified Responses to Stimuli-Responsive Materials. *ACS Macro Lett.* **2014**, *3*, 298−304.

(6) Yardley, R. E.; Kenaree, A. R.; Gillies, E. R. Triggering Depolymerization: Progress and Opportunities for Self-Immolative Polymers. *Macromolecules* **2019**, *52*, 6342−6360.

(7) McBride, R. A.; Gillies, E. R. Kinetics of Self-Immolative Degradation in a Linear Polymeric System: Demonstrating the Effect of Chain Length. *Macromolecules* **2013**, *46*, 5157−5166.

(8) Parkatzidis, K.; Wang, H. S.; Truong, N. P.; Anastasaki, A. Recent Developments and Future Challenges in Controlled Radical Polymerization: A 2020 Update. *Chem* **2020**, *6*, 1575−1588.

(9) Worch, J. C.; Dove, A. P. 100th Anniversary of Macromolecular Science Viewpoint: Toward Catalytic Chemical Recycling of Waste (and Future) Plastics. *ACS Macro Lett.* **2020**, *9*, 1494−1506.
(10) Fagnani, D. E.; Tami, J. L.; Copley, G.; Clemons, M. N.; Getzler, Y. D. Y. L.; McNeil, A. J. 100th Anniversary of Macromolecular Science Viewpoint: Redefining Sustainable Polymers. *ACS Macro Lett.* **2021**, 41−53.
(11) Sagi, A.; Weinstain, R.; Karton, N.; Shabat, D. Self-Immolative Polymers. *J. Am. Chem. Soc.* **2008**, *130*, 5434−5435.
(12) Odian, G. *Principles of Polymerization*; 4th Ed.; John Wiley & Sons, Inc.: 2004.
(13) Dainton, F. S.; Ivin, K. J. Some thermodynamic and kinetic aspects of addition polymerisation. *Q. Rev., Chem. Soc.* **1958**, *12*, 61−92.
(14) Sawada, H. Chapter 3. Thermodynamics of Radical Polymerization. *J. Macromol. Sci., Polym. Rev.* **1969**, *3*, 357−386.
(15) Penczek, S.; Kaluzynski, K. Thermodynamic and Kinetic Polymerizability. *Polym. Sci.: Compr. Ref.* **2012**, *4*, 5−20.
(16) Dainton, F. S.; Ivin, K. J. Reversibility of the Propagation Reaction in Polymerizatoin Processes and its Manifestation in the Phenomenon of a 'Ceiling Temperature'. *Nature* **1948**, *162*, 705−707.
(17) Penczek, S.; Moad, G. Glossary of terms related to kinetics, thermodynamics, and mechanisms of polymerization (IUPAC Recommendations 2008). *Pure Appl. Chem.* **2008**, *80*, 2163−2193.
(18) Sano, Y.; Konishi, T.; Sawamoto, M.; Ouchi, M. Controlled radical depolymerization of chlorine-capped PMMA via reversible activation of the terminal group by ruthenium catalyst. *Eur. Polym. J.* **2019**, *120*, 109181.
(19) Ito, K.; Hashizuka, Y.; Yamashita, Y. Equilibrium Cyclic Oligomer Formation in the Anionic Polymerization of iε-Caprolactone. *Macromolecules* **1977**, *10*, 821−824.
(20) Heuvelsland, A. J. Method for producing 1,4-dioxane. US Patent No. 4,764,626A. Aug. 16, 1988
(21) Plesch, P. H.; Westermann, P. H. The Polymerization of 1,3-Dioxolane. I. Structure of the Polymer and Thermodynamics of Its Formation. In *Journal of Polymer Science Part C: Polymer Symposia*; New York: Wiley Subscription Services, Inc., A Wiley Company: 1967; *16* (7), 3837−3843, DOI: 10.1002/polc.5070160724.
(22) Lomakin, S. M.; Brown, J. E.; Breese, R. S.; Nyden, M. R. An investigation of the thermal stability and char-forming tendency of cross-linked poly(methyl methacrylate). *Polym. Degrad. Stab.* **1993**, *41*, 229−243.
(23) Godiya, C. B.; Gabrielli, S.; Materazzi, S.; Pianesi, M. S.; Stefanini, N.; Marcantoni, E. Depolymerization of waste poly(methyl methacrylate) scraps and purification of depolymerized products. *J. Environ. Manage.* **2019**, *231*, 1012−1020.
(24) Al-Salem, S. M.; Lettieri, P.; Baeyens, J. Recycling and recovery routes of plastic solid waste (PSW): a review. *Waste Manage.* **2009**, *29*, 2625−2643.
(25) Gilsdorf, R. A.; Nicki, M. A.; Chen, E. Y.-X. High chemical recyclability of vinyl lactone acrylic bioplastics. *Polym. Chem.* **2020**, *11*, 4942−4950.
(26) Moens, E. K. C.; De Smit, K.; Marien, Y. W.; Trigilio, A. D.; Van Steenberge, P. H. M.; Van Geem, K. M.; Dubois, J.-L.; D'Hooge, D. R. Progress in Reaction Mechanisms and Reactor Technologies for Thermochemical Recycling of Poly(methyl methacrylate). *Polymers* **2020**, *12*, 1667.
(27) *Polymer Handbook*; 4th Ed.; Brandrup, J., Immergut, E. H., Grulke, E. A. Eds.; Wiley: 2003.
(28) Kashiwagi, T.; Inaba, A.; Brown, J. E.; Hatada, K.; Kitayama, T.; Masuda, E. Effects of weak linkages on the thermal and oxidative degradation of poly(methyl methacrylates). *Macromolecules* **1986**, *19*, 2160−2168.
(29) Manring, L. E.; Sogah, D. Y.; Cohen, G. M. Thermal degradation of poly(methyl methacrylate). 3. Polymer with head-to-head linkages. *Macromolecules* **1989**, *22*, 4652−4654.
(30) Manring, L. E. Thermal degradation of poly(methyl methacrylate). 2. Vinyl-terminated polymer. *Macromolecules* **1989**, *22*, 2673−2677.
(31) Manring, L. E. Thermal Degradation of Poly(methyl methacrylate). 4. Random Side-Group Scission. *Macromolecules* **1986**, *19*, 3304−2168.
(32) Manring, L. E. Thermal degradation of saturated poly(methyl methacrylate). *Macromolecules* **1988**, *21*, 528−530.
(33) Grant, D. H.; Bywater, S. Thermal Depolymerization of Polymethylmethacrylate in Diphenylether Solution. *Trans. Faraday Soc.* **1963**, *59*, 2105−2112.
(34) Bywater, S.; Black, P. E. Thermal Depolymerization of Polymethyl Methacrylate and Poly-α-methylstyrene in Solution in Various Solvents[1,2]. *J. Phys. Chem.* **1965**, *69*, 2967−2970.
(35) Flanders, M. J.; Gramlich, W. M. Reversible-addition fragmentation chain transfer (RAFT) mediated depolymerization of brush polymers. *Polym. Chem.* **2018**, *9*, 2328−2335.
(36) Czech, Z.; Agnieszka, K.; Ragańska, P.; Antosik, A. Thermal stability and degradation of selected poly(alkyl methacrylates) used in the polymer industry. *J. Therm. Anal. Calorim.* **2014**, *119*, 1157−1161.
(37) Matyjaszewski, K.; Xia, J. Atom Transfer Radical Polymerization. *Chem. Rev.* **2001**, *101*, 2921−2990.
(38) Matyjaszewski, K. *Controlled Radical Polymerization: State of the Art in 2008*; American Chemical Society: 2009; *1023*, 3−13.
(39) Moad, G.; Chong, Y. K.; Mulder, R.; Rizzardo, E.; Thang, S. H. *New Features of the Mechanism of RAFT Polymerization*; American Chemical Society: 2009; *1024*, 3−18.
(40) Nicolas, J.; Guillaneuf, Y.; Lefay, C.; Bertin, D.; Gigmes, D.; Charleux, B. Nitroxide-mediated polymerization. *Prog. Polym. Sci.* **2013**, *38*, 63−235.
(41) Krys, P.; Matyjaszewski, K. Kinetics of Atom Transfer Radical Polymerization. *Eur. Polym. J.* **2017**, *89*, 482−523.
(42) Fischer, H. The Persistent Radical Effect: A Principle for Selective Radical Reactions and Living Radical Polymerizations. *Chem. Rev.* **2001**, *101*, 3581−3610.
(43) Jakubowski, W.; Min, K.; Matyjaszewski, K. Activators Regenerated by Electron Transfer for Atom Transfer Radical Polymerization of Styrene. *Macromolecules* **2006**, *39*, 39−45.
(44) Jakubowski, W.; Min, K.; Tang, W.; Huang, J.; Braunecker, W. A.; Tsarevsky, N. V.; Matyjaszewski, K. Diminishing catalyst concentration in atom transfer radical polymerization with reducing agents. *Proc. Natl. Acad. Sci.* **2006**, *103*, 15309−15314.
(45) Matyjaszewski, K. Atom Transfer Radical Polymerization (ATRP): Current Status and Future Perspectives. *Macromolecules* **2012**, *45*, 4015−4039.
(46) Lloyd, D. J.; Nikolaou, V.; Collins, J.; Waldron, C.; Anastasaki, A.; Bassett, S. P.; Howdle, S. M.; Blanazs, A.; Wilson, P.; Kempe, K.; Haddleton, D. M. Controlled aqueous polymerization of acrylamides and acrylates and *"in situ"* depolymerization in the presence of dissolved CO_2. *Chem. Commun.* **2016**, *52*, 6533−6536.
(47) Raus, V.; Čadová, E.; Starovoytova, L.; Janata, M. ATRP of POSS Monomers Revisited: Toward High-Molecular Weight Methacrylate−POSS (Co)Polymers. *Macromolecules* **2014**, *47*, 7311−7320.
(48) Sheiko, S. S.; Dobrynin, A. V. Architectural Code for Rubber Elasticity: From Supersoft to Superfirm Materials. *Macromolecules* **2019**, *52*, 7531−7546.
(49) Cong, Y.; Vatankhah-Varnosfaderani, M.; Karimkhani, V.; Keith, A. N.; Leibfarth, F. A.; Martinez, M. R.; Matyjaszewski, K.; Sheiko, S. S. Understanding the Synthesis of Linear−Bottlebrush−Linear Block Copolymers: Toward Plastomers with Well-Defined Mechanical Properties. *Macromolecules* **2020**, *53*, 8324−8332.
(50) Daniel, W. F.; Burdynska, J.; Vatankhah-Varnoosfaderani, M.; Matyjaszewski, K.; Paturej, J.; Rubinstein, M.; Dobrynin, A. V.; Sheiko, S. S. Solvent-free, supersoft and superelastic bottlebrush melts and networks. *Nat. Mater.* **2016**, *15*, 183−189.
(51) Martinez, M. R.; Cong, Y.; Sheiko, S. S.; Matyjaszewski, K. A Thermodynamic Roadmap for the Grafting-through Polymerization of $PDMS_{11}MA$. *ACS Macro Lett.* **2020**, *9*, 1303−1309.
(52) Tasic, A.; Pergal, M.; Antić, M.; Antić, V. Synthesis, structure and thermogravimetric analysis of α,ω-telechelic polydimethylsiloxanes of low molecular weight. *J. Serb. Chem. Soc.* **2017**, *82*, 1395−1416.

(53) Camino, G.; Lomakin, S. M.; Lazzari, M. Polydimethylsiloxane thermal degradation Part 1. Kinetic aspects. *Polymer* **2001**, *42*, 2395−2402.
(54) Granel, C.; Dubois, P.; Jérôme, R.; Teyssié, P. Controlled Radical Polymerization of Methacrylic Monomers in the Presence of a Bis(ortho-chelated) Arylnickel(II) Complex and Different Activated Alkyl Halides. *Macromolecules* **1996**, *29*, 8576−8582.
(55) Moineau, G.; Minet, M.; Dubois, P.; Teyssié, P.; Senninger, T.; Jérôme, R. Controlled Radical Polymerization of (Meth)acrylates by ATRP with $NiBr_2(PPh_3)_2$ as Catalyst. *Macromolecules* **1999**, *32*, 27−35.
(56) Camilo, A. P. R.; de Almeida, P.; Petzhold, C. L.; Felisberti, M. I. Thermal degradation of poly(alkyl methacrylate) synthesized via ATRP using 2,2,2-tribromoethanol as initiator. *Polym. Degrad. Stab.* **2018**, *158*, 1−13.
(57) Jackson, A. T.; Bunn, A.; Priestnall, I. M.; Borman, C. D.; Irvine, D. J. Molecular spectroscopic characterisation of poly(methyl methacrylate) generated by means of atom transfer radical polymerisation (ATRP). *Polymer* **2006**, *47*, 1044−1054.
(58) Borman, C. D.; Jackson, A. T.; Bunn, A.; Cutter, A. L.; Irvine, D. J. Evidence for the low thermal stability of poly(methyl methacrylate) polymer produced by atom transfer radical polymerisation. *Polymer* **2000**, *41*, 6015−6020.
(59) Szczepaniak, G.; Piątkowski, J.; Nogaś, W.; Lorandi, F.; Yerneni, S. S.; Fantin, M.; Ruszczyńska, A.; Enciso, A. E.; Bulska, E.; Grela, K.; Matyjaszewski, K. An isocyanide ligand for the rapid quenching and efficient removal of copper residues after Cu/TEMPO-catalyzed aerobic alcohol oxidation and atom transfer radical polymerization. *Chem. Sci.* **2020**, *11*, 4251−4262.
(60) Bhanu, V. A.; Kishore, K. Role of oxygen in polymerization reactions. *Chem. Rev.* **1991**, *91*, 99−117.
(61) Martinez, M. R.; Sobieski, J.; Lorandi, F.; Fantin, M.; Dadashi-Silab, S.; Xie, G.; Olszewski, M.; Pan, X.; Ribelli, T. G.; Matyjaszewski, K. Understanding the Relationship between Catalytic Activity and Termination in photoATRP: Synthesis of Linear and Bottlebrush Polyacrylates. *Macromolecules* **2020**, *53*, 59−67.
(62) Fairservice, W. I.; Fairservice, W. H. Effects of salts of metals on vinyl polymerization. Part 1.—Polymerization of methyl methacrylate in presence of cupric chloride. *Trans. Faraday Soc.* **1965**, *61*, 1206−1215.
(63) Ribelli, T. G.; Konkolewicz, D.; Bernhard, S.; Matyjaszewski, K. How are radicals (re)generated in photochemical ATRP? *J. Am. Chem. Soc.* **2014**, *136*, 13303−13312.
(64) Hong, H.; Matyjaszewski, K. ARGET ATRP of 2-(Dimethylamino)ethyl Methacrylate as an Intrinsic Reducing Agent. *Macromolecules* **2008**, *41*, 6868−6870.
(65) Kwak, Y.; Matyjaszewski, K. ARGET ATRP of methyl methacrylate in the presence of nitrogen-based ligands as reducing agents. *Polym. Int.* **2009**, *58*, 242−247.
(66) Kaur, A.; Ribelli, T. G.; Schroder, K.; Matyjaszewski, K.; Pintauer, T. Properties and ATRP activity of copper complexes with substituted tris(2-pyridylmethyl)amine-based ligands. *Inorg. Chem.* **2015**, *54*, 1474−1486.
(67) Lanzalaco, S.; Fantin, M.; Scialdone, O.; Galia, A.; Isse, A. A.; Gennaro, A.; Matyjaszewski, K. Atom Transfer Radical Polymerization with Different Halides (F, Cl, Br, and I): Is the Process "Living" in the Presence of Fluorinated Initiators? *Macromolecules* **2017**, *50*, 192−202.
(68) Elsen, A. M.; Burdyńska, J.; Park, S.; Matyjaszewski, K. Active Ligand for Low PPM Miniemulsion Atom Transfer Radical Polymerization. *Macromolecules* **2012**, *45*, 7356−7363.

https://doi.org/10.1021/acs.macromol.1c00415
Macromolecules 2021, 54, 5526−5538